Peer-reviewed version available at *Atmosphere* **2020**, *11*, 956; doi:10.3390/atmos11090956

Article

Drought modulated boreal forest fire occurrence and linkage with La Nina events in Altai Mountains, Northwest China

Chunming Shi [1], Ying Liang [2,]* , Cong Gao [1], Fengjun Zhao [3], Qiuhua Wang [4] and Lifu Shu [3,]*

[1] College of Global Change and Earth System Science, Beijing Normal University, Beijing 100875, China; chunming.shi@gmail.com (C.S.); gaocong@mail.bnu.edu.cn (C.G.)
[2] Xinjiang Academy of forestry Sciences, Urumqi 830000, Xinjiang Province, China; liangying0421@126.com
[3] Research Institute of Forest Ecology, Environment and Protection, Chinese Academy of Forestry; Forest Protection Laboratory of National Forestry and Grassland Administration, Beijing 100091, China; zhaofj@caf.ac.cn
[4] College of Civil Engineering, Southwest Forestry University, Kunming 650224, Yunnan Province, China; qhwang2010@swfu.edu.cn
* Correspondence: liangying0421@126.com (L.Y.); slfhxk@126.com (L.S.)

Abstract: Warming-induced drought stress and El Nino associated summer precipitation failure are responsible for increased forest fire intensities of tropical and temperate forests in Asia and Australia. However, both effects are unclear for boreal forests, the largest biome and carbon stock over land. Here we combined fire frequency, burned area and climate data in the Altai boreal forests, the southmost extension of Siberia boreal forest into China, and explored their link with ENSO (El Nino and South Oscillation). Surprisingly, both summer drought severity and fire occurrence have shown significant ($P<0.05$) teleconnections with La Nina events of the previous year, and therefore provide an important reference for forest fire prediction and prevention in Altai. Despite a significant warming trend, the increased moisture over Altai has largely offset the effect of warming-induced drought stress, and lead to an insignificant fire frequency trend in the last decades, and largely reduced burned area since the 1980s. The reduced burned area could also benefit from the fire suppression efforts and greatly increased investment in fire prevention since 1987.

Keywords: boreal forest; forest fire; ENSO; Altai Mountain

---

1. Introduction

Climate warming is faster at higher latitudes and altitudes [1-3]. Boreal forest, the largest biome and living carbon stock on land, has therefore experienced a faster warming rate than global mean level, and an unprecedented large fire disturbance over the past 10,000 years [4], mainly due to increased lighting ignition in association with warming [5-8], fire season extension [9,10], and higher fuel aridity [11,12]. Forest fire plays a key role in dominating the structure, succession, and function of the boreal forests [13-14], and releases a large amount of organic carbon into the atmosphere, potentially transferring boreal forest from net carbon sink to net source [15,16]. The forest fire emitted CO_2, black carbon and aerosols have aggravated global warming [17], which in turn increased the fire risk [18,19]. Although great anthropogenic suppression efforts have been taken globally, the observed and projected forest fire intensity is still increasing significantly over the globe in the 21st century [20-23].

Superimposed on the warming-forced forest fire increasing trend, internal variabilities inherent in the climate system have modulated fire regime at interannual to decadal time scale, e.g. ENSO (El Nino-South Oscillation), shifting between warm (El Nino) and cold (La Nina) phases, was considered one of the main sources of inter-annual climate variabilities. At longer timescale, PDO (Pacific Decadal Oscillation), an ENSO like climate variability but varies at inter-decadal timescale, was shown to modulate ENSO's impacts through in-phase (overlapping) or out-phase (counteract) with ENSO [24-26]. Both ENSO and PDO, showing close teleconnections with precipitations and temperature variabilities [27-29], have modulated drought conditions [30-32], and therefore forest fire occurrence over a large part of the Asian and American continents [23]. The frequency of extreme El Nino and la Nina events are projected to increase with global warming [33-35], substantially elevate future forest fire risks.

The effects of ENSO and PDO on forest fire variabilities have been widely explored over the tropical and temperate forests, e.g., the combination of cold ENSO (La Nina) and PDO phases were closely related to anomalous high fire occurrence in west coast forests of North America [36-38]. In contrast, the dry condition in association with warm ENSO (El Nino) and PDO phases have led to significantly increased forest fire intensity in most China [39], Southeast Asia [40], central to eastern America [23,41,42], southeast Australia [43,44], and tropical rain forests [45]. A warm ENSO-warm PDO combination has greatly increased fire risks, frequency and burned area in the boreal forests in North America and Northeast China [25, 46-49], and wildfire emissions in the northern high latitudes [50]. However, the impacts of ENSO and PDO on the boreal forest fire of none-monsoonal regions, especially in inland Asia is still unclear. The connections of La Nina events with high fire risks of boreal forest have not been found.

In this study, we have constructed a dataset combining fire frequency, burned areas of the boreal forest in Northwest China. The linkage of fire data with ENSO and long-term climate trends and the teleconnection between local climate and ENSO were explored as well.

2. Data and method

2.1. Study region

This research focused on forest fires in the Altay Prefecture of Xinjiang Province, China, the most Northwest corner of China (grey area in the top left insert of Fig.1), which is adjacent to three countries of Mongolia, Russia, and Kazakhstan. The boreal forest in the study region is the southmost extension of Sibiria boreal forest into China. The annual mean temperature and total precipitations are 2.4 ºC and 200.4 mm respectively. 62.5% of precipitation falls in May-September (here defined as summer) when almost all forest fire occurs. The large snow cover before May and after September has largely suppressed the fire occurrence.

2.2. Fire and climate data

May-September fire numbers and burned area data spanning 1960-2018 were obtained from individual forest administrations of seven counties of Altai, and were then averaged to represent the mean fire frequency of Altai Prefecture. 0.5° resolved monthly climate data, including temperature, precipitation, and self-calibrating Palmer Drought Severity Index (scPDSI) were extracted from the Climate Research Unit (CRU) TS 4.03 dataset and averaged over a rectangle of 45-49°N, 85-91°E to estimate the mean climate condition of Altai. The One-month Standardised Precipitation-Evapotranspiration Index (SPEI1) and monthly relative humidity (RH) data (black triangles in Fig.1) were downloaded from Spanish National Research Council (CSIC) and meteorological stations of the seven counties, respectively. NINO3 and PDO indices derived from ERSST v5 datasets were obtained.

The years with fire occurrence and SPEI1 above and bellow the 95% distribution limits were defined as the years of most frequent fire and drought stress, respectively. The coincidence of the extreme years was tested. In order to explore the connection of drought severity and fire occurrence, correlation analysis was conducted using summer fire frequency and moisture indicators. Monthly NINO3 and PDO data were correlated to summer fire frequency to determine the key season of teleconnection and possible time-lag effect, the same analysis between key-season NINO3 and summer moisture indices was conducted to explore the mechanisms underlining the teleconnection.

Preprints (www.preprints.org) | NOT PEER-REVIEWED | Posted: 1 August 2020 doi:10.20944/preprints202008.0001.v1

Peer-reviewed version available at Atmosphere 2020, 11, 956; doi:10.3390/atmos11090956

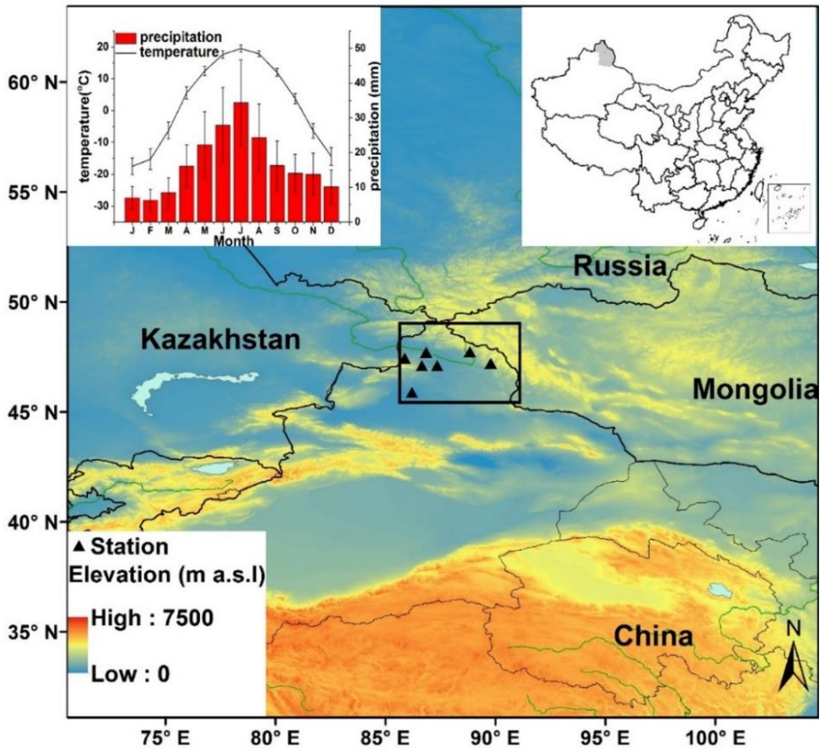

Figure 1. Meteorological stations are indicated with black triangles; Grey shading of the top right insert shows the Altai Prefecture. The black rectangle is the study area (45-49°N, 85-91°E). The top left insert is the Walter Lieth diagram of the study region, the temperature (black curve) and precipitation (red bars) are the regional averaged data of CRU TS4.03 dataset.

3. Results

3.1. Linkage of fire and moisture variability

The mean correlation coefficient of the summer fire frequency records of the seven counties reaches 0.49 (1960-2018, Figure A1), suggesting a synchronous variation of fire occurrence and reasonability pooling these data. Six years with the most frequent fire occurrence (Year-f) and the largest drought stress (Year-d) were identified, respectively. We found 4 out of 6 Year-f (1962, 1963, 1974 and 1982), and the two years with the largest burned areas (1962 and 1974) coincided with Year-d. Four out of 6 Year-f occurred before 1987, since when a great fire suppression effort has been carried out in China. The R between summer fire frequency and SPEI1 reaches 0.46 (1960-2018, P<0.001), showing the possible link of drought severity and fire occurrence. The trend of fire frequency is insignificant (1960-2018, slope= 0.45±1.45 /year, P=0.55). Exceptional large burned areas were recorded in 1962 and 1974 (4.6 and 18.1×103 hm2, respectively), which are coincided with two driest years over 1960-2018 (lowest SPEI values in 1962 and 1974). Burned area has never exceed 3×103 hm2 since the 1980s. Even with comparable drought condition and fire frequency in 2008, the burned area has not reached similar level of 1962 and 1974.

 doi:10.20944/preprints202008.0001.v1

Peer-reviewed version available at *Atmosphere* **2020**, *11*, 956; doi:10.3390/atmos11090956

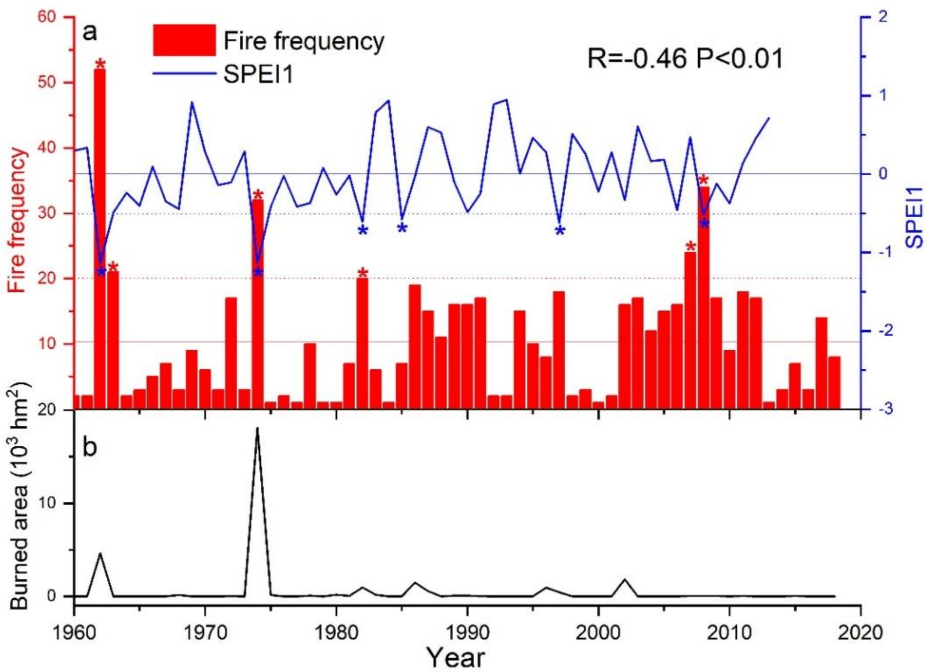

Figure 2. a: Summer (May-Sep) fire frequency (red column) and SPEI1(solid blue line), the horizontal solid lines are the mean values, the dashed red and blue lines indicate the limits of 95% significant deviation from the mean value. Extreme frequent fire and dry years were defined as above and below these limits and marked by red and blue stars, respectively; **b**: annual summer burned area.

The negative correlation between summer fire frequency and moisture indices, including precipitation, SPEI1, scPDSI and Relative Humidity are all significant above 95% level (Fig. 2 R=-0.42, -0.46, -0.26 and -0.45; P< 0.01, 0.01, 0.05 and 0.01, respectively), suggesting a drought-induced fire occurrence in Altai region. A significant correlation was not found for fire frequency and temperature records, regardless of minimum, mean, or maximum temperatures.

Preprints (www.preprints.org) | NOT PEER-REVIEWED | Posted: 1 August 2020 doi:10.20944/preprints202008.0001.v1

Peer-reviewed version available at Atmosphere 2020, 11, 956; doi:10.3390/atmos11090956

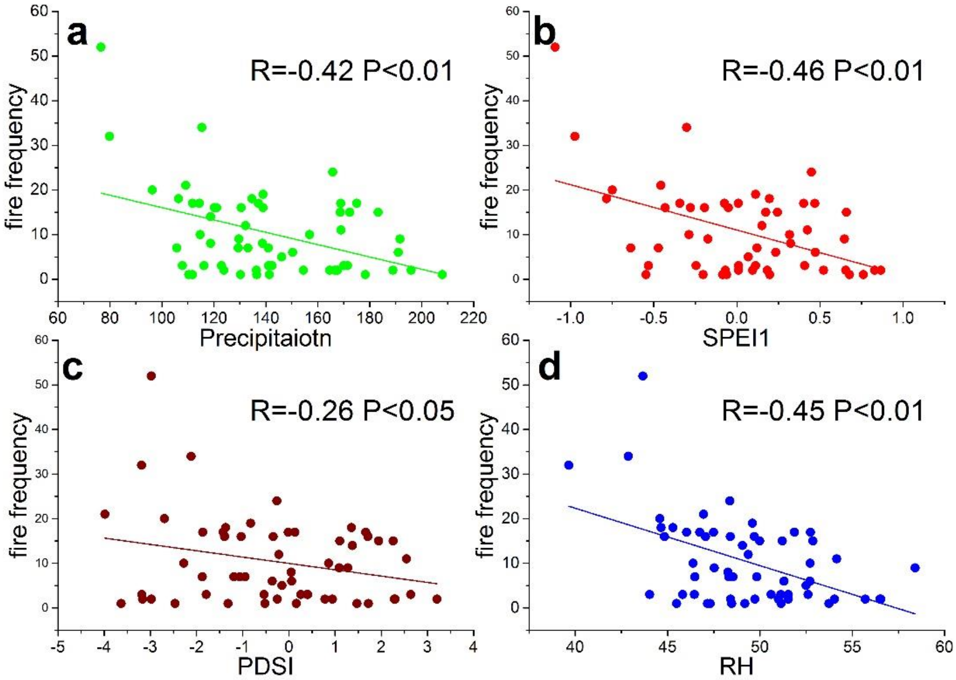

Figure 3. Scatter plot with correlation coefficients between summer fire frequency and moisture variability of the study region. a precipitation; b SPEI1; c scPDSI; d relative humidity.

3.2. Teleconnection of ENSO/PDO and local moisture variabilities

Figure 4 shows July-October NINO3 and October-November PDO of the previous year are significantly ($P<0.05$) and negatively correlated with fire frequency of the current summer. Although insignificant, the correlation coefficients are all negative from Previous December to the current May. All these results imply a persistent teleconnection between previous Sea Surface Temperature (SST) of the eastern tropical Pacific Ocean and summer Altai fire-climate variabilities.

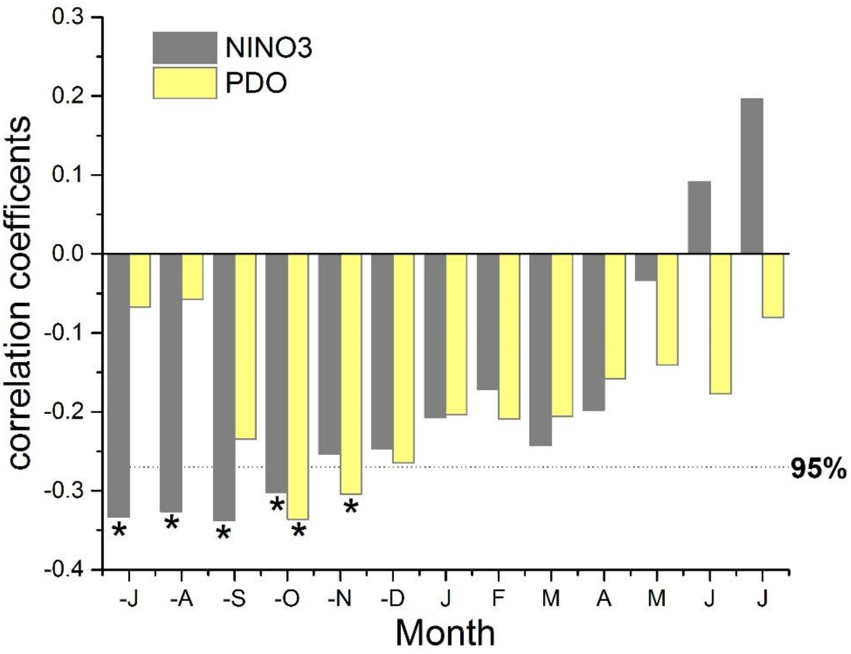

 doi:10.20944/preprints202008.0001.v1

Peer-reviewed version available at *Atmosphere* **2020**, *11*, 956; doi:10.3390/atmos11090956

Figure 4. Correlation coefficients of monthly NINO3/PDO and summer fire frequency from July of the previous year to July of the current year (1960-2018), horizontal dashed line is the 95% significant level.

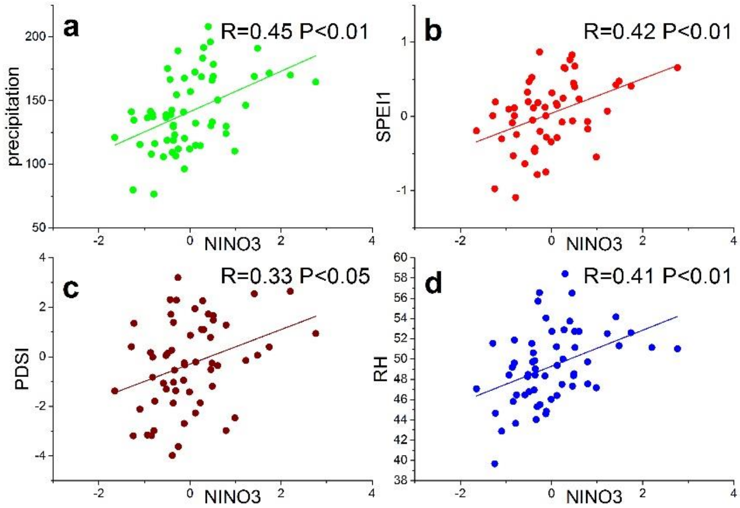

Figure 5. Scatter plot with correlation coefficients between NINO3 average over July-October of the previous year and summer moisture variability of the current year. a precipitation; b SPEI1; c scPDSI; d relative humidity.

To understand the mechanisms underlying the teleconnection between ENSO and local climate, correlation analysis of NINO3 and moisture indices was conducted and presented in Figure 5. All the 4 moisture indices have shown significantly positive R with NINO3 index (R=0.45, 0.42, 0.33 and 0.41; P<0.01, 0.01, 0.05 and 0.01 for precipitation, SPEI1, scPDSI and RH, respectively), suggesting a previous El Nino event could lead to high summer moisture availability in Altai, and vice versa. The spatial correlation between July-October NINO3 index of the previous year and summer precipitation, SPEI1 and scPDSI are all significant (P<0.05) over the study region (Fig. 6a-6c). In addition, summer Altai RH shows significant coherence (P<0.05) with previous July-October SST over the eastern tropical Pacific Ocean (Fig. 6d), where the SST anomalies define NINO3 index.

Preprints (www.preprints.org) | NOT PEER-REVIEWED | Posted: 1 August 2020 doi:10.20944/preprints202008.0001.v1

Peer-reviewed version available at Atmosphere 2020, 11, 956; doi:10.3390/atmos11090956

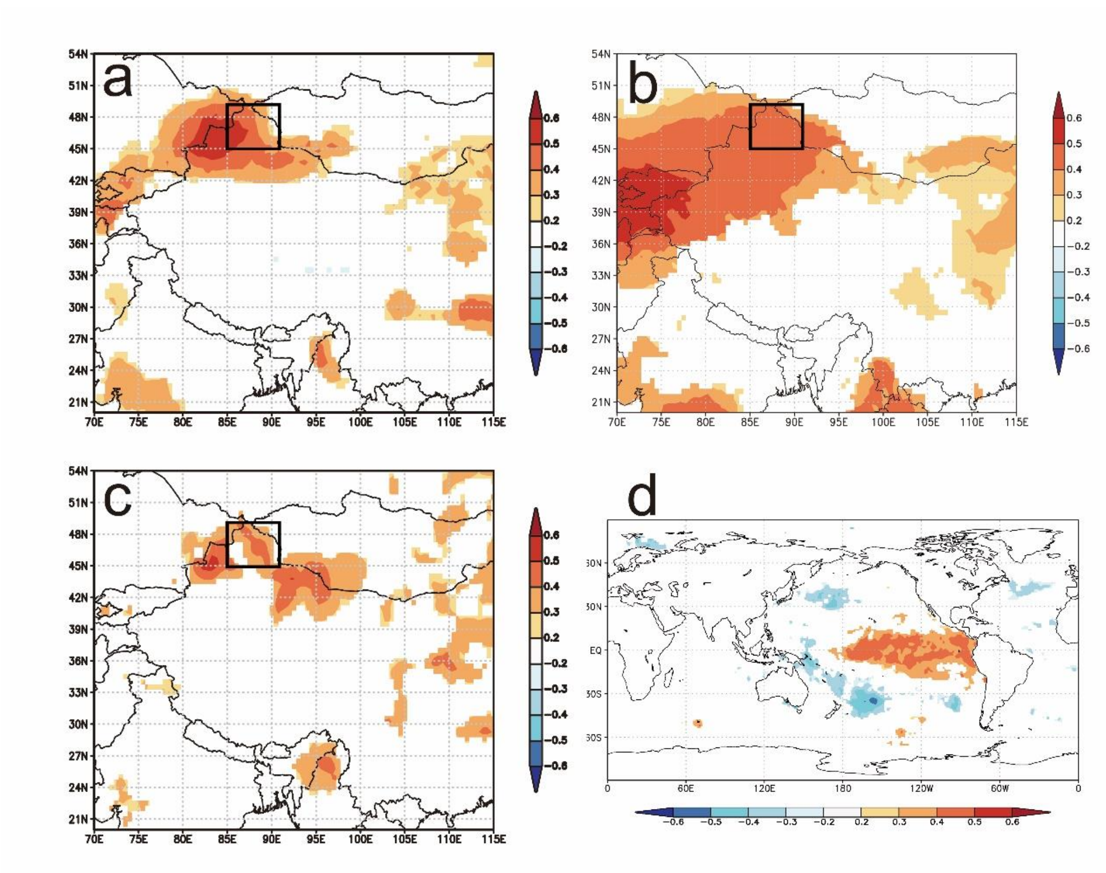

Figure 6. Spatial correlation coefficients of July-October NINO3 index of the previous year and summer moisture indicators, including a precipitation, b SPEI1 and c scPDSI. Black rectangles are the study region. Subplot d is spatial correlation coefficients of summer Altai RH and July-October global SST of the previous year. Only parts with R value <0.05 were shown.

4. Discussion

4.1. Regional climate trends, fire frequency and burned area

High drought severity can increase the aridity of fuels, and elevate forest fire frequency and area burned [51-53]. Warming itself and the associated increase in drought stress, extreme hot events, and fire season length are supposed to raise fire risks as well. [54,55]. Global-change-type drought, also termed as warming-induced drought stress, have contributed to a large part of burned area and fire risk increase over dry areas [53,56]. However, despite a significant summer warming (0.28±0.026 ºC/decade P<0.001, Figure A2a), the trend of annual summer fire frequency is insignificant in Altai.

In this study, both coincidences of frequent fire and extremely dry years, and correlation analysis have shown a significant connection between drought stress and fire occurrence in Altai (Fig. 2 and 3). Among the moisture indices used, scPDSI and SPEI1 are showing a slight and significant wet trend (Figure A2b and A2d), whereas precipitation is increasing as well but statistically insignificant (Figure A2c).

The ambiguous fire frequency trend, and largely reduced burned area could also due to the significant moistening trend along with warming, and to strong fire suppression efforts and greatly increased investment in fire prevention since 1987.

4.2. Teleconnections of La Nina events and drought stress in Altai

The El Nino events, defined as anomalously high SST over the eastern tropical Pacific, can lead to a following warmer SSTs over the Northwest Pacific and tropical Indian Oceans [57,58], which further reduced the land-ocean thermal gradient, delayed the onset of the East Asian Summer Monsoon (EASM) and South Asian Summer Monsoon (SASM), and weakened monsoon intensities

Preprints (www.preprints.org) | NOT PEER-REVIEWED | Posted: 1 August 2020 doi:10.20944/preprints202008.0001.v1

Peer-reviewed version available at Atmosphere 2020, 11, 956; doi:10.3390/atmos11090956

[59,60]. Thus El Nino is usually responsible for inter-annual drought stress and fire occurrence in many monsoonal regions [61-63].

On the contrary, we find the dry conditions (low precipitation, SPEI1 and scPDSI) of Altai are significantly associated with previous La Nina events (low NINO3) (Fig. 5 and 6). The same findings have been reported for summer precipitation in Xinjiang, and the teleconnections and time-lag effect was interpreted with an atmospheric bridge theory: with a cooler Indian Ocean SST in association with La Nina events, South Asian High (SAH) exhibits a northward extension due to the decreasing geopotential height in its southern flank, and lead to a barotropic high-pressure anomaly and less precipitation over Northwest China [60]. The significant teleconnections between previous La Nina events and high drought severity/fire occurrence can provide important knowledge for long-term forest fire prediction in Altai.

4.3. Comparison with ENSO's impact in other studies

Previous studies have shown that fire risks and severities in boreal forests are higher following El Nino events in Canada and Northeast China [25,44]. Moreover, fire activities of boreal forests were usually characterized by large multidecadal variabilities, which were modulated by long-term climate dynamics in the Pacific and Atlantic sectors, such as PDO and AMO (Atlantic Multidecadal Oscillation) [25,44,46,47,64]. For the first time, we have identified fire occurrence of boreal forests is lacking of long-term variability, and tele-connected with La Nina rather than El Nino. At interannual time scale, El Nino events contribute to extremely warm and dry conditions, are responsible for more wildfires in many regions of the world [38-41,43], whereas La Nina associated fires can only be found in a few regions, such as west America [35].

Author Contributions: Conceptualization, C.S.; methodology, C.S.; software, C.S.; validation, C.S., Y.L. and L.S.; formal analysis, C.S.; investigation, C.S.; resources, C.S.; data curation, Y.L.; writing—original draft preparation, C.S.; writing—review and editing, C.G., F.Z. and Q.W.; visualization, C.S.; supervision, C.S.; project administration, C.S.; funding acquisition, C.S., Q.W. and L.S. All authors have read and agreed to the published version of the manuscript.

Funding: This research was funded by National Key Research and Development Plan(2017YFD0600106) and the Natural Science Foundation of China (31971667, 31570645 and 31660210).

Acknowledgments: The authors would like to acknowledge the Science and Technology Ministry and National Natural Science Foundation of China for their financial support as part of the statutory works.

Conflicts of Interest: The authors declare no conflict of interest.

Appendix

Peer-reviewed version available at Atmosphere 2020, 11, 956; doi:10.3390/atmos11090956

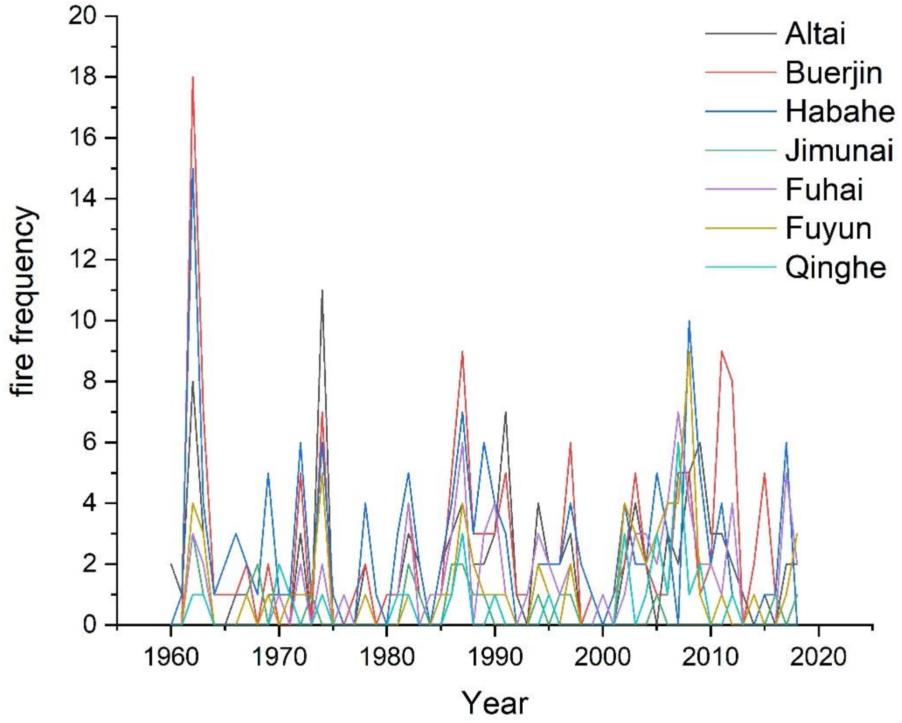

209

210 **Figure A1.** summer forest fire frequency of the 7 counties of Altay prefecture

211

Peer-reviewed version available at Atmosphere 2020, 11, 956; doi:10.3390/atmos11090956

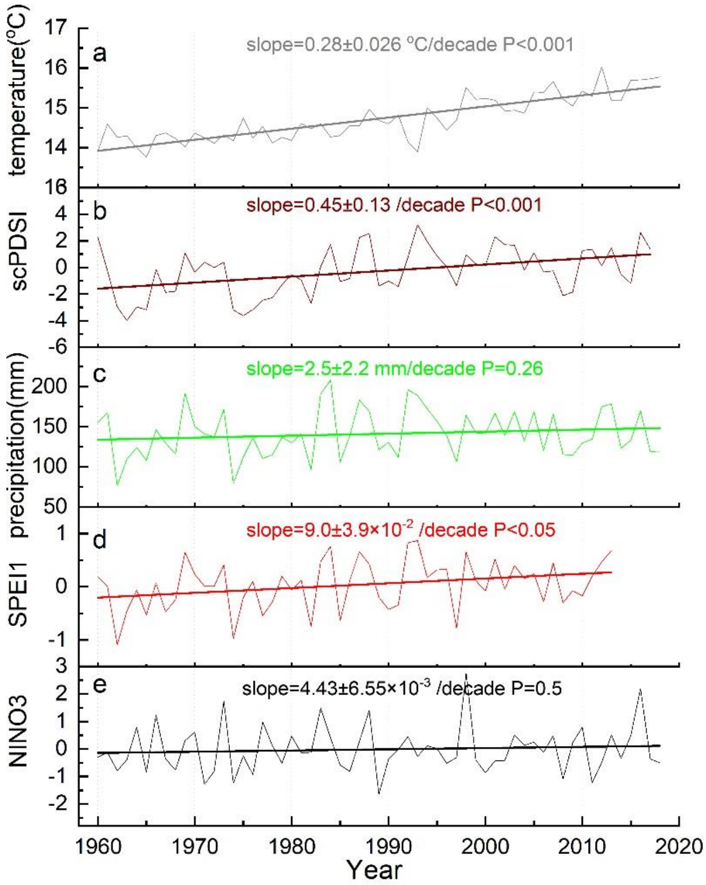

Figure A2. summer climate trend over the study region, including temperature (a), scPDSI (b). precipitation (c), SPEI1(d) and July-October NINO3 index of the previous year (e)

References

1. Jones, P.D.; New M; Parker D.E.; Martin, S.; Rigor, I.G. Surface air temperature and its changes over the past 150 years. *Rev. Geophys.* **1999**, *37*, 173-199.
2. Screen, J.A.; Simmonds, I. The central role of diminishing sea ice in recent Arctic temperature amplification. *Nature* **2010**, *464*, 1334-1337.
3. Pepin, N.; Bradley, R.S.; Diaz, H.F.; Baraer, M.; Caceres, E.B.; Forsythe, N.; Fowler, H.; Greenwood, G.; Hashmi, M.Z.; Liu, X.D.; et al. Elevation-dependent warming in mountain regions of the world. *Nat. Clim. Change* **2015**, *5*, 424-430.
4. Kelly, R.; Chipman, M.L.; Higuera, P.E.; Stefanova, I.; Brubaker, L.B.; Hu, F.S. Recent burning of boreal forests exceeds fire regime limits of the past 10,000 years. *P. Natl. Acad. Sci. Usa* **2013**, *110*, 13055-13060.
5. Price, C.; Rind, D. Possible implications of global climate change on global lightning distributions and frequencies. *J.Geophys. Res.* **1994**, *99*, 10823.
6. Romps, D.M.; Seeley, J.T.; Vollaro, D.; Molinari, J. Projected increase in lightning strikes in the United States due to global warming. *Science* **2014**, *346*, 851-854.
7. Veraverbeke, S.; Rogers, B.M.; Goulden, M.L.; Jandt, R.R.; Miller, C.E.; Wiggins, E.B. and Randerson, J.T. Lightning as a major driver of recent large fire years in North American boreal forests. *Nat. Clim. Change* **2017**, *7*, 529.
8. Hanes, C.C.; Wang, X.; Jain, P.; Parisien, M.; Little, J.M.; Flannigan, M.D. Fire-regime changes in Canada over the last half century. *Can. J. Forest Res.* **2019**, *49*, 256-269.
9. Westerling, A.L. Increasing western US forest wildfire activity: sensitivity to changes in the timing of spring. *Philos T. R. Soc B.* **2016**, *371*, 20150175.

Preprints (www.preprints.org) | NOT PEER-REVIEWED | Posted: 1 August 2020 doi:10.20944/preprints202008.0001.v1

Peer-reviewed version available at *Atmosphere* **2020**, *11*, 956; doi:10.3390/atmos11090956

10. Westerling, A.L.; Hidalgo, H.G.; Cayan, D.R.; Swetnam, T.W. Warming and earlier spring increase western US forest wildfire activity. *Science* **2006**, *313*, 940-943.
11. Portier, J.; Gauthier, S.; Leduc, A.; Arseneault, D.; Bergeron, Y. Fire Regime along Latitudinal Gradients of Continuous to Discontinuous Coniferous Boreal Forests in Eastern Canada. *Forests* **2016**, 7.
12. Gonzalez, M.E.; Gomez-Gonzalez, S.; Lara, A.; Garreaud, R.; Diaz-Hormazabal, I. The 2010-2015 Megadrought and its influence on the fire regime in central and south-central Chile. *Ecosphere* **2018**, *9*, e02300.
13. Overpeck, J.T.; Rind, D.; Goldberg, R. Climate-induced changes in forest disturbance and vegetation. *Nature* **1990**, *343*, 51-53.
14. Johnstone, J.F.; Hollingsworth, T.N.; Chapin, F.S.I.; Mack, M.C. Changes in fire regime break the legacy lock on successional trajectories in Alaskan boreal forest. *Global Change Biol.* **2010**, *16*, 1281-1295.
15. Bond-Lamberty, B.; Peckham, S.D.; Ahl, D.E.; Gower, S.T. Fire as the dominant driver of central Canadian boreal forest carbon balance. *Nature* **2007**, *450*, 89.
16. Walker, X.J.; Baltzer, J.L.; Cumming, S.G.; Day, N.J.; Ebert, C.; Goetz, S.; Johnstone, J.F.; Potter, S.; Rogers, B.M.; Schuur, E.A.G.; et al. Increasing wildfires threaten historic carbon sink of boreal forest soils. *Nature* **2019**, *572*, 520.
17. Randerson, J.T.; Liu, H.; Flanner, M.G.; Chambers, S.D.; Jin, Y.; Hess, P.G.; Pfister, G.; Mack, M.C.; Treseder, K.K.; Welp, L.R.; et al. The impact of boreal forest fire on climate warming *Science* **2006**, *314*, 1130-1132.
18. Oris, F.; Asselin, H.; Ali, A.A.; Finsinger, W.; Bergeron, Y. Effect of increased fire activity on global warming in the boreal forest. *Environ. Rev.* **2014**, *22*, 206-219.
19. van der Werf, G.R.; Randerson, J.T.; Giglio, L.; van Leeuwen, T.T.; Chen, Y.; Rogers, B.M.; Mu, M.; van Marle, M.J.E.; Morton, D.C.; Collatz, G.J.; et al. Global fire emissions estimates during 1997-2016. *Earth Syst. Sci. Data* **2017**, *9*, 697-720.
20. Turetsky, M.R.; Kane, E.S.; Harden, J.W.; Ottmar, R.D.; Manies, K.L.; Hoy, E.; Kasischke, E.S. Recent acceleration of biomass burning and carbon losses in Alaskan forests and peatlands. *Nat. Geosci.* **2011**, *4*, 27-31.
21. Westerling, A.L.; Turner, M.G.; Smithwick, E.A.H.; Romme, W.H.; Ryan, M.G. Continued warming could transform Greater Yellowstone fire regimes by mid-21st century. *P. Natl Acad Sci Usa* **2011**, *108*, 13165-13170.
22. Flannigan, M.; Cantin, A.S.; de Groot, W.J.; Wotton, M.; Newbery, A.; Gowman, L.M. Global wildland fire season severity in the 21st century. *Forest. Ecol. Manag.* **2013**, *294*, 54-61.
23. Jolly, W.M.; Cochrane, M.A.; Freeborn, P.H.; Holden, Z.A.; Brown, T.J.; Williamson, G. J.; Bowman, D. M. J. S. Climate-induced variations in global wildfire danger from 1979 to 2013. *Nat. Commun.* **2015**, *6*, 7537.
24. Schoennagel, T.; Veblen, T.T.; Romme, W.H.; Sibold, J.S.; Cook, E.R. Enso and pdo variability affect drought-induced fire occurrence in Rocky Mountain subalpine forests. *Ecol. Appl*. **2005**, *15*, 2000-2014.
25. Krishnamurthy, L.; Krishnamurthy, V.; Influence of PDO on South Asian summer monsoon and monsoon-ENSO relation. *Clim. Dynam.* **2014**, *42*, 2397-2410.
26. Yao, Q.; Brown, P.M.; Liu, S.; Rocca, M. E.; Trouet, V.; Zheng, B.; Chen, H.; Li, Y.; Liu, D.; Wang, X. Pacific-Atlantic Ocean influence on wildfires in northeast China (1774 to 2010). *Geophys Res Lett.* **2017**, *44*, 1025-1033.
27. Gershunov, A.; Barnett, T.P. ENSO influence on intraseasonal extreme rainfall and temperature frequencies in the contiguous United States: Observations and model results. *J. Climate* **1998**, *11*, 3062-3065.
28. Lluch-Cota, D.B.; Wooster, W.S.; Hare, S.R. Sea surface temperature variability in coastal areas of the Northeastern Pacific related to the El Nino-Southern Oscillation and the Pacific Decadal Oscillation. *Geophys. Res. Lett.* **2001**, *28*, 2029-2032.
29. Wu, R.; Yang, S.; Liu, S.; Sun, L.; Lian, Y.; Gao, Z. Changes in the relationship between Northeast China summer temperature and ENSO. *J. Geophys. Res.-Atmos.* **2010**, *115*, D21107.
30. McCabe, G.J.; Palecki, M.A.; Betancourt, J.L. Pacific and Atlantic Ocean influences on multidecadal drought frequency in the United States. *P. Natl Acad Sci Usa* **2004**, *101*, 4136-4141.
31. Mo, K.C.; Schemm, J.E.; Yoo, S. Influence of ENSO and the Atlantic Multidecadal Oscillation on Drought over the United States. *J. Climate* **2009**, *22*, 5962-5982.
32. Wen, N.; Liu, Z.; Li, L. Direct ENSO impact on East Asian summer precipitation in the developing summer. *Clim. Dynam.* **2019**, *52*, 6799-6815.
33. Timmermann, A.; Oberhuber, J.; Bacher, A.; Esch, M.; Latif, M.; Roeckner, E. Increased El Nino frequency in a climate model forced by future greenhouse warming. *Nature* **1999**, *398*, 694-697.

Preprints (www.preprints.org) | NOT PEER-REVIEWED | Posted: 1 August 2020 doi:10.20944/preprints202008.0001.v1

Peer-reviewed version available at *Atmosphere* **2020**, *11*, 956; doi:10.3390/atmos11090956

34. Cai, W.; Borlace, S.; Lengaigne, M.; van Rensch, P.; Collins, M.; Vecchi, G.; Timmermann, A.; Santoso, A.; McPhaden, M.J.; Wu, L.; et al. Increasing frequency of extreme El Nino events due to greenhouse warming. *Nat. Clim. Change* **2014**, *4*, 111-116.
35. Cai, W.; Wang, G.; Santoso, A.; McPhaden, M.J.; Wu, L.; Jin, F.; Timmermann, A.; Collins, M.; Vecchi, G.; Lengaigne, M.; et al. Increased frequency of extreme La Nina events under greenhouse warming. *Nat. Clim. Change* **2015**, *5*, 132-137.
36. Sibold, J.S.; Veblen, T.T. Relationships of subalpine forest fires in the Colorado Front Range with interannual and multidecadal-scale climatic variation. *J. Biogeogr.* **2006**, *33*, 833-842.
37. Schoennagel, T.; Veblen, T.T.; Kulakowski, D.; Holz, A. Multidecadal climate variability and climate interactions affect subalpine fire occurrence, Western Colorado (USA). *Ecology* **2007**, *88*, 2891-2902.
38. Sherriff, R.L.; Veblen, T.T. Variability in fire-climate relationships in ponderosa pine forests in the Colorado Front Range. *Int J. Wildland Fire* **2008**, *17*, 50-59.
39. Tian, X.; Shu, L.; Ali, F. The Affection of ENSO and Macula on Forest Fires in China. *World Forestry Res.* **2003**, *16*, 22-25.
40. van der Werf, G.R.; Randerson, J.T.; Collatz, G.J.; Giglio, L.; Kasibhatla, P.S.; Arellano, A. F.; Olsen, S.C.; Kasischke, E.S. Continental-scale partitioning of fire emissions during the 1997 to 2001 El Nino/La Nina period. *Science* **2004**, *303*, 73-76.
41. Hessl, A.E.; McKenzie, D.; Schellhaas, R. Drought and Pacific Decadal Oscillation linked to fire occurrence in the inland Pacific Northwest. *Ecol. Appl.* **2004**, *14*, 425-442.
42. Margolis, E.Q.; Swetnam, T.W. Historical fire-climate relationships of upper elevation fire regimes in the south-western United States. *Int J. Wildland Fire* **2013**, *22*, 588-598.
43. Power, S.; Casey, T.; Folland, C.; Colman, A.; Mehta, V. Inter-decadal modulation of the impact of ENSO on Australia. *Clim. Dynam.* **1999**, *15*, 319-324.
44. Mariani, M.; Fletcher, M.S.; Holz, A.; Nyman, P. ENSO controls interannual fire activity in southeast Australia. *Geophys. Res. Lett.* **2016**, *43*, 10891-10900.
45. Siegert, F.; Ruecker, G.; Hinrichs, A.; Hoffmann, A.A. Increased damage from fires in logged forests during droughts caused by El Nino. *Nature* **2001**, *414*, 437-440.
46. Macias-Fauria, M.; Johnson, E.A. Large-scale climatic patterns control large lightning fire occurrence in Canada and Alaska forest regions. *J. Geophys. Res.-Biogeo.* **2006**, *111*, G04008.
47. Macias-Fauria, M.; Johnson, E.A. Climate and wildfires in the North American boreal forest. *Philos. Trans. R. Soc. Lond.; B; Biol. Sci.* **2008**, *363*, 2317-2329.
48. Meyn, A.; Taylor, S.W.; Flannigan, M.D.; Thonicke, K.; Cramer, W. Relationship between fire; climate oscillations, and drought in British Columbia, Canada, 1920-2000. *Glob. Chang. Biol.* **2010**, *16*, 977-989.
49. Harvey, J.E.; Smith, D.J. Interannual climate variability drives regional fires in west central British Columbia, Canada. *J. Geophys. Res.-Biogeo.* **2017**, *122*, 1759-1774.
50. Monks, S.A.; Arnold, S.R.; Chipperfield, M.P. Evidence for El Nino-Southern Oscillation (ENSO) influence on Arctic CO interannual variability through biomass burning emissions *Geophys. Res. Lett.* **2012**, *39*, L14804.
51. Russo, A.; Gouveia, C.M.; Pascoa, P.; DaCamara, C.C.; Sousa, P.M.; Trigo, R.M. Assessing the role of drought events on wildfires in the Iberian Peninsula. *Agr. Forest Meteorol.* **2017**, *237*, 50-59.
52. Taufik, M.; Torfs, P.J.J.F.; Uijlenhoet, R.; Jones, P.D.; Murdiyarso, D.; Van Lanen, H.A.J. Amplification of wildfire area burnt by hydrological drought in the humid tropics. *Nat. Clim. Change* **2017**, *7*, 428.
53. Kodandapani, N.; Parks, S.A. Effects of drought on wildfires in forest landscapes of the Western Ghats, India. *Int J. Wildland Fire* **2019**, *28*, 431-444.
54. Crockett, J.L.; Westerling, A.L. Greater Temperature and Precipitation Extremes Intensify Western US Droughts, Wildfire Severity; and Sierra Nevada Tree Mortality. *J. Climate* **2018**, *31*, 341-354.
55. Ruffault. J.; Curt, T.; Martin-StPaul, N.K.; Moron, V.; Trigo, R.M. Extreme wildfire events are linked to global-change-type droughts in the northern Mediterranean. *Nat. Hazard Earth Sys.* **2018**, *18*, 847-856.
56. Gudmundsson, L.; Rego, F.C.; Rocha, M.; Seneviratne, S.I. Predicting above normal wildfire activity in southern Europe as a function of meteorological drought. *Environ. Res. Lett.* **2014**, *9*, 084008.
57. Chan, J.; Zhou, W. PDO; ENSO and the early summer monsoon rainfall over south China. *Geophys. Res. Lett.* **2005**, *32*, L08810.
58. Yang, J.; Liu, Q.; Xie, S.; Liu, Z.; Wu, L. Impact of the Indian Ocean SST basin mode on the Asian summer monsoon. *Geophys. Res. Lett.* **2007**, *34*, L02708.
59. Ju, J.H.; Slingo, J. The Asian Summer Monsoon and ENSO. *Q. J. Roy. Meteor. Soc.* **1995**, *121*, 1133-1168.

Preprints (www.preprints.org) | NOT PEER-REVIEWED | Posted: 1 August 2020 doi:10.20944/preprints202008.0001.v1

Peer-reviewed version available at *Atmosphere* **2020**, *11*, 956; doi:10.3390/atmos11090956

60. Wang, B.; Wu, R.G.; Lau, K.M. Interannual variability of the Asian summer monsoon: Contrasts between the Indian and the western North Pacific-east Asian monsoons. *J. Climate* **2001**, *14*, 4073-4090.
61. Cleary, D.; Grill, A. Butterfly response to severe ENSO-induced forest fires in Borneo. *Ecol. Entomol.* **2004**, *29*, 666-676.
62. Lu, B.; Li, H.; Wu, J.; Zhang, T.; Liu, J.; Liu, B.; Chen, Y.; Baishan, J. Impact of El Nino and Southern Oscillation on the summer precipitation over Northwest China. *Atmos. Sci. Lett.* **2019**, *20*, e928.
63. Novitasari, N.; Sujono, J.; Harto, S.; Maas, A.; Jayadi, R. Drought Index for Peatland Wildfire Management in Central Kalimantan; Indonesia During El Nino Phenomenon. *J. Disa. Res.* **2019**, *14*, 939-948.
64. Mori, A.S. Climatic variability regulates the occurrence and extent of large fires in the subalpine forests of the Canadian Rockies. *Ecosphere* **2011**, *2*, 1-20.